Received: 6 March 2019 | Revised: 6 February 2020 | Accepted: 17 February 2020

DOI: 10.1002/gea.21788

RESEARCH ARTICLE

Geoarchaeology An International Journal WILEY

Lithic artifact assemblage transport and microwear modification in a fluvial setting: A radio frequency identification tag experiment

Wei Chu[1] | Robert Hosfield[2]

[1]Faculty of Arts and Humanities, Institute for Early and Prehistory, University of Cologne, Cologne, Germany

[2]Department of Archaeology, School of Archaeology, Geography and Environmental Science (SAGES), University of Reading, Reading, UK

Correspondence
Wei Chu, Faculty of Arts and Humanities, Institute for Early and Prehistory, University of Cologne, Weyertal 125, 50923 Cologne, Germany.
Email: wchu@uni-koeln.de

Scientific editing by Steve Kuhn

Funding information
Universität zu Köln, Grant/Award Numbers: INST 216/596-2, Post doc grant

Abstract

River processes are widely assumed to have impacted the integrity of lithic assemblages when artifacts are found in fluvial sediments, but the specifics of these influences remain largely unknown. We conducted a real-world experiment to determine how the initial stages of fluvial entrainment affected lithic artifact assemblages. We inserted replica artifacts with radio frequency identification tags into a gravel-bedded river in Wales (UK) for seven months and related their transport distances to their morphology and the recorded streamflow. In addition, nine artifacts were recovered at the end of the experiment and analyzed for microwear traces. In sum, our results show that in a gravel-bedded river with a mean discharge of 5.1 m^3/s, artifact length and width were the main variables influencing artifact transport distances. The experiment also resulted in characteristic microwear traces developing on the artifacts over distances of 485 m or less. These results emphasize the multifaceted nature of alluvial site formation processes in a repeatable experiment and highlight new ways to identify the transport of replica Paleolithic material.

KEYWORDS

experimental archaeology, fluvial dynamics, Paleolithic, RFID, taphonomy, use-wear

1 | INTRODUCTION

Lithic artifacts are a main source of information for reconstructing the movements, technological behaviors, and diets of ancient hominins. Their morphology, location, and spatial associations provide archaeologists with key data sets to test hypotheses. Paleolithic artifacts are frequently found embedded within Pleistocene fluvial deposits, reflecting both anthropogenic behavior and landscape taphonomy, thus making the latter crucial repositories for information on past hominins (van den Biggelaar, Balen, Kluiving, Verpoorte, & Alink, 2017; Bridgland & White, 2014; Bridgland et al., 2006; Chauhan et al., 2017; de la Torre, Benito-Calvo, & Proffitt, 2018; Westaway, Bridgland, Sinha, & Demir, 2009). At the same time, experimental archaeology is a valuable instrument in the researcher's investigatory toolkit (Eren et al., 2016; Lin, Rezek, & Dibble, 2018) and has been used periodically over the last half-century to determine questions such as whether lithic artifacts in a river behave as normal clasts or whether their unique shape and anthropogenic insertion points substantially modify their entrainment, movement, deposition, and abrasion.

Field experiments were first initiated by Isaac (1967) and Schick (1986), to understand the impact of hydrological sorting of lithic assemblages in ephemeral rivers in East Africa. Their findings, that smaller artifacts were selectively transported downstream, were elaborated upon by Petraglia and Nash (1987) who showed that a number of factors including the tempo, magnitude, and duration of fluvial events play

important roles in transport. Other experiments (e.g., Harding, Gibbard, Lewin, Macklin, & Moss, 1987) focused on gravel-bedded rivers where Paleolithic artifacts are also commonly preserved and found that larger replica handaxes placed in the Ystwyth River conformed to the established paradigm that smaller artifacts travel farther and demonstrated that contact with the gravel bedload elicited characteristic surface and edge damage and subsequent weight loss as a result. Later experiments in gravel-bedded rivers have produced conflicting data. Other experiments (Chambers, 2004; Hosfield & Chambers, 2004a, 2005; Hosfield, Chambers, Macklin, Brewer, & Sear, 2000) found that flake scatters tended to stay together during the initial transport stages (>10 m) and that size had little impact on their movement due to periodic "trapping" of artifacts within the gravel bed. Transported artifacts were also characterized by widened ridges, edge microflaking, and impact marks (Hertzian cones). At another gravel-bedded river, Chu (2016) found that artifact length, width, and depositional locations were significantly correlated to transport distances.

This past research, in addition to a number of laboratory experiments (see Chu, 2016 for extensive review), has highlighted that local fluvial environments, river velocity, artifact size, and shape all influence initial artifact entrainment and deposition that can, in turn, obscure original artifact discard locations, modify morphology, alter assemblage composition, and bias artifacts' final orientations (Bertran, Bordes, Todisco, & Vallin, 2017; Bunn et al., 1980; Byers, Hargiss, & Finley, 2015; Ditchfield, 2016; Hosfield, 2011; Hosfield & Chambers, 2004a; Petraglia & Nash, 1987; Schick, 1987). However, there are limits to these past experiments, most notably that they have commonly relied on visually marked tracers (e.g., painted stones) that have hampered recovery due to postentrainment burial.

In combination, these previous studies have suggested that a number of main points remain unresolved and/or require further study:

1. How do artifact metrics affect their transport, entrainment, and deposition in the variety of river types known from Pleistocene archives (e.g., meandering, braided; cold-climate, and temperate)? What is the best predictor of transport distance (if any)?
2. Where do artifacts typically become deposited in fluvial environments (if anywhere)?
3. How are artifacts dispersed in fluvial environments?
4. Under what fluvial conditions are artifact orientations altered? Do they orient in situ or only if they are transported, or both?
5. What, if any, are the relationships between transport distances and artifact damage and modifications?

Here, we present an experiment using radio frequency identification (RFID) tagged replica lithic artifacts inserted into a gravel-bedded, meandering river in a temperate, and mid-latitude environment. RFID tagging improves artifact recovery allowing for enhanced postentrainment analyses (Houbrechts et al., 2015; Lamarre, 2005). The method is derived from geomorphological studies and supports high recovery rates throughout the project area (Hassan & Bradley, 2017). The approach also allows for artifact surfaces to be largely unmodified (e.g., it avoids the use of artifact marking with paint to enable recovery and identification), permitting artifact modifications such as edge damage and microwear to be meaningfully studied. It also generates accurate artifact transport distances that can be linked to artifact size measurements, streamflow characteristics, and morphological modifications. Combined, it allows artifact positional changes to be monitored over time, and for potential distinctions between use-wear/retouch and river modifications to be explored.

1.1 | Background

Field experiments were carried out on a 1.14 km section of the River Ystwyth in Llanafan, County Ceredigion, UK between 52.3313°N, −3.8959°W and 52.3288°N, −3.9093°W, 14 km upstream from the Pont Llolwyn gauging station (Figure 1). The River Ystwyth flows westward into Cardigan Bay at Aberystwyth and drains the west slopes of Plynlimon in the Cambrian Mountains. The length of the main river is 33 km covering a catchment area of 191 km^2 (Foulds, Griffiths, Macklin, & Brewer, 2014). The surrounding catchment terrain has a maximum height of 612 m above ordnance datum and is primarily comprised of grassland mainly used for forestry and sheep husbandry. During the experiment, the river generated a mean annual river discharge of 5.1 m^3/s and a maximum daily mean discharge of 72.6 m^3/s (measured at the Pont Llolwyn gauging station; 52.374642°N, −4.072693°W).

For the past 200 years, the section of the river has been characterized by aggradation related to historical mining. Predominantly aggrading regimes are likely to have been common during the transitional periods of Pleistocene climate cycles (after Bridgland, 2000), when sediment-supply rates were increased due to cold/cool climates with reduced vegetation cover (Lewin, Bradley, & Macklin, 1983). As a result of the recent aggradations, the current valley floor is filled with Holocene alluvium, dominated by sandy gravels predominantly derived from local impermeable Silurian shales and gritstones, with a high proportion of disc- and blade-shaped clasts with a mean flatness of 0.44 (c/b; Graham, Reid, & Rice, 2005). The coarse-grained river sediments have a median diameter (D_{50}) of 40 ± 10 mm (min 17 mm and max 53 mm) and a 95th percentile grain diameter of (D_{95}) 96 ± 27 mm (min 43 and max 140; Graham et al., 2005; Graham, Rice, & Reid, 2005). Finer sedimentary units are present throughout, associated with bars, riverbends, and floodplain surfaces (Hosfield & Chambers, 2005). The banks in the study area are not channelized and are characterized by active bar development and the regular transport of bed materials. The project area was likely unaffected by significant foot or animal traffic during the period of the experiment, as the land is often cordoned off and/or inaccessible due to high vegetation.

This project area was chosen for three main reasons:

1. The frequent mobility of clasts within the gravel-bedded system.

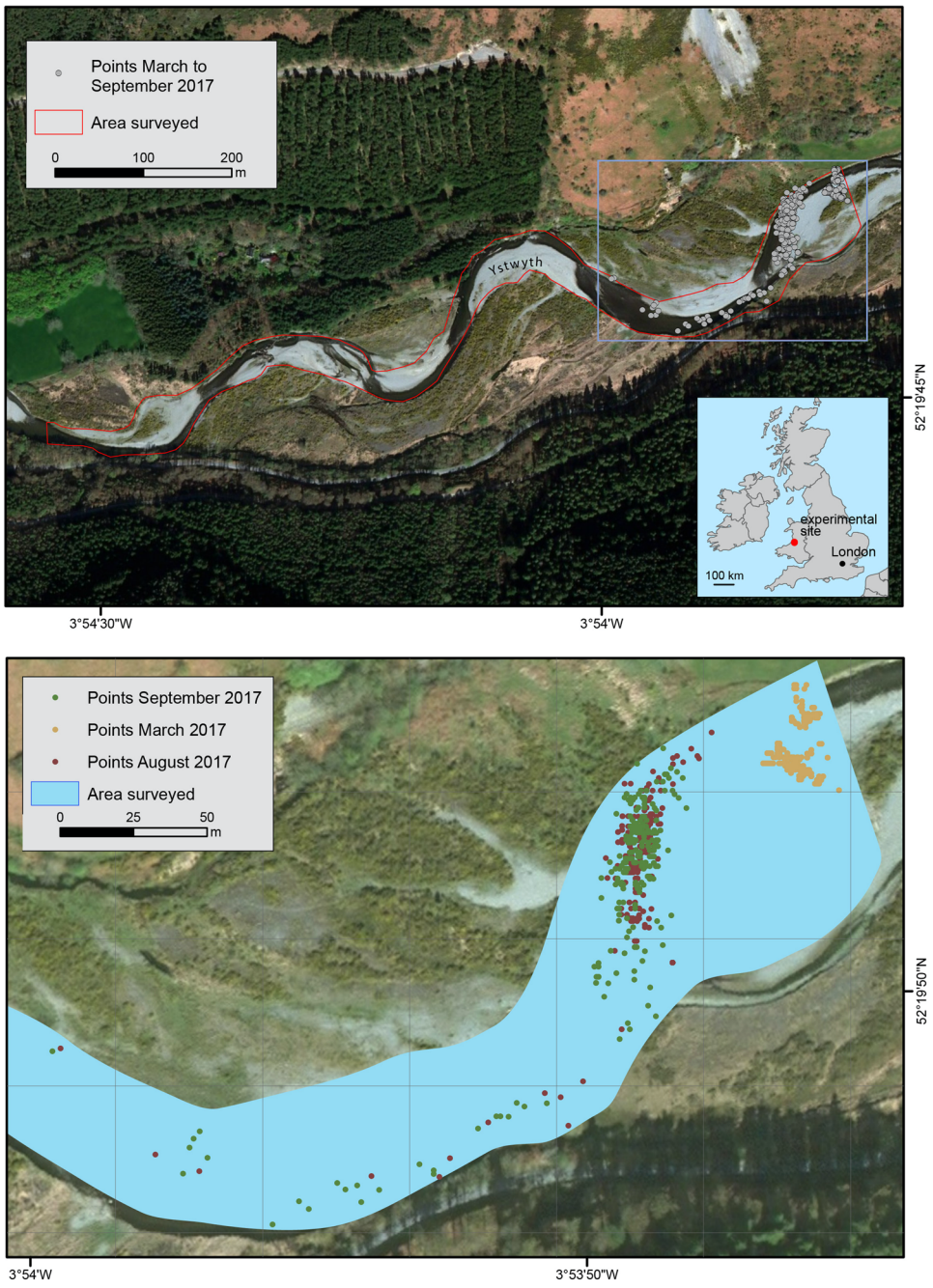

FIGURE 1 The project area of the fluvial experiments showing (top) the location and survey area and (bottom) location of artifacts during the surveys. Note: The river flows from east to west (Map data: Google, DigitalGlobe) [Color figure can be viewed at wileyonlinelibrary.com]

2. The catchment's topography makes the Yswyth a flashy river; prone to rapid rises and falls in level depending on rainfall, thus promoting artifact entrainment and deposition and facilitating fieldwork.
3. The river has been used in previous artifact transport and geomorphological studies, providing comparative and contextual data (Brewer, Johnstone, & Macklin, 2009; Brewer, Maas, & Macklin, 2001; Harding et al., 1987; Hosfield & Chambers, 2004a, 2004b; Hosfield et al., 2000).

2 | MATERIALS AND METHODS

Replica artifacts were produced by experienced knappers, covering different Paleolithic forms including handaxes, blades, flakes, and cores (Table 1; Figure 2) from a range of European raw materials (partly from Lengyel and Chu, 2016). In addition, the handaxes were previously used in a well-documented experiment to butcher fallow deer (*Dama dama*; Machin, Hosfield, & Mithen, 2007). Artifacts were individually wrapped in aeroplast after production to preserve the

TABLE 1 Descriptive statistics of artifacts used in this experiment

	Udden–Wentworth (Wentworth, 1922) grain size scheme	*n*	Minimum	Maximum	Mean	*SD*
Length (mm)		568	11.99	151.04	56.61	23.54
	Large cobble	7	128.30	151.04	136.39	9.78
	Small cobble	150	85.19	127.70	85.19	18.13
	Very coarse pebble	371	63.97	32.11	46.56	8.85
	Coarse pebble	40	24.42	31.94	29.65	2.02
Width (mm)		568	12.31	114.50	38.11	17.07
	Small cobble	48	64.02	114.50	78.57	12.54
	Very coarse pebble	268	32.05	63.65	43.70	8.37
	Coarse pebble	242	16.36	31.96	24.88	4.22
	Medium pebble	10	12.31	16.00	14.59	1.06
Thickness (mm)		568	1.02	53.80	14.01	8.44
	Very coarse pebble	22	32.01	53.80	39.11	6.64
	Coarse pebble	155	16.03	31.74	21.76	4.42
	Medium pebble	249	8.05	15.94	11.54	2.33
	Fine pebble	124	4.04	7.95	6.12	1.10
	Very fine pebble	17	2.12	3.97	3.44	0.49
	Very coarse sand	1	1.02	1.02	1.02	N/A
Weight (g)		568	0.70	546.00	34.67	62.38

Abbreviation: *SD*, standard deviation.

integrity of their surfaces and edges. A 15 × 4 mm niche was then removed from the center of the artifacts with a water-jet cutter that incises material with a focused jet of water mixed with abrasive grit. An HPT12 Passive Integrative Transponder tag (Biomark; 9 × 2 mm; 134.2 kHz) with a unique serial code was inserted into the niche and fixed with epoxy resin. The maximum length, maximum width, and maximum thickness of the replica artifacts were recorded to the nearest 1 mm (Andrefsky, 2005). Weight was recorded to the nearest 0.1 g. Artifacts were then photographed on their dorsal and ventral sides.

Field experiments were conducted between March 13–15, 2017, August 3–6, 2017, and again in September 15–18, 2017. During the first field visit, a single "scatter" of 454 artifacts of differing lithologies was emplaced in a regular grid on a riverbank, where artifacts were positioned 25 cm apart from each other with a randomly oriented long-axis. During the second visit, another 114 artifacts were emplaced in a single pile (25 cm radius) simulating a knapping scatter.

Artifact locations were recorded with a *Biomark HPR Plus Reader* using a *BP Plus portable antenna* that has an integrated global positioning system (GPS) unit (horizontal accuracy of ±3 m) and is able to detect tags underwater and/or beneath gravels from a distance of up to 45 cm (Cassel, Piégay, & Lavé, 2017). During subsequent monitoring visits, the surface of the project area (Figure 1) was scanned with the RFID antenna in 2 m strips traversing the river channel and floodplain to ensure the entire riverbed and banks were appropriately covered (Chapuis, Bright, Hufnagel, & MacVicar, 2014). When found, artifact locations, the date, time, and GPS coordinates were automatically recorded and if possible, orientation was recorded with a transit compass. Where visible, artifacts were recovered at the end of the experiment.

Artifact locations, measurements, and orientation values were later compiled and imported into QGIS (2.18). Equivalent artifact location points (pre- and posttransport) were matched. These were then converted to distances by creating a vector file of artifact travel distances using the R package "riverdist" which simulates the most parsimonious artifact travel path through a river. All subsequent statistical analyses were performed with SPSS 22.

Nine transported artifacts were further selected for microwear study based on their morphology and distance traveled (between 0 and 485 m). They were cleaned with 10% HCL solution for 20 min, rinsed with water, and immersed in a 10% KOH solution for 20 min. Artifacts were then analyzed with a stereomicroscope (Nikon SMZ-2T and Leica M80 with magnifications ×7.5–60) and a metallographic microscope (Leica DM6000M and Leica DM2700P, with magnifications ×100 and ×200). Photographs were taken using a digital microscope camera (Leica DFC450 and Leica MC120HD). For an extensive description of the microwear methodology, see van Gijn (1989, 2010).

3 | RESULTS

3.1 | Do artifact dimensions predict transport distance?

The individual relationships between artifact dimensions, elongation (length/width), refinement (width/thickness; Iovita & McPherron, 2011),

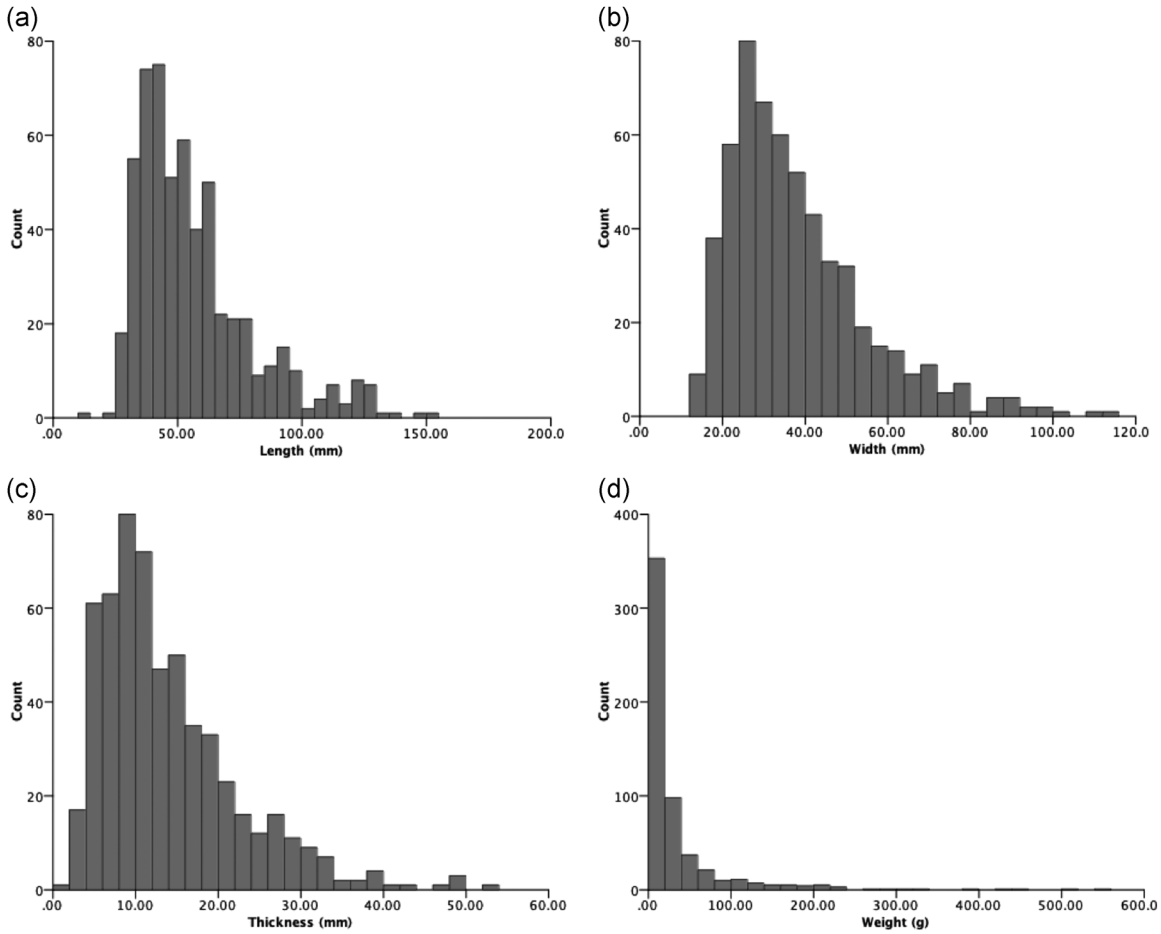

FIGURE 2 Artifact size distributions used in this experiment: (a) by length; (b) by width; (c) by thickness; and (d) by weight

and transport distances were tested with bootstrapped single linear regressions. The data used in these analyses were artifact measurements and the total transport distances for all artifacts between March and September 2017. The experimental artifacts provided a robust data set to explore the effects of artifact measurements on transport distances during the initial stages of fluvial reworking since they were transported up to 485 m, were exposed to the same maximum hydrological flows and were inserted along the same gravel bar. Figure 3 displays scatter plots reporting the results of bootstrapped linear regressions comparing transport distance with maximum length, maximum width, maximum thickness, weight, elongation, and refinement and Table 2 displays the distances traveled by clast size and clast shape. Both artifact maximum length (R^2 = .010, F(1, 416) = 4.339, p < .038) and artifact maximum width (R^2 = .020, F(1, 416) = 8.540, p < .004) statistically significantly affected artifact transport distance.

Because data were not always normally distributed, potential differences between artifact transport distances across subsamples of artifact size categories were tested with a Kruskal–Wallis H test, which indicated nonsignificant differences between the subsamples (Figure 4a; Table 3; χ^2 [3] = 7.377, p = .061). To test artifact transport data subdivided by artifact shape categories, a Kruskal–Wallis H was also performed and indicated nonsignificant differences by the subsamples (Figure 4b; χ^2 [3] = 2.574, p = .462). Overall, statistical analysis did not indicate significant differences between the total distances moved by artifacts in different size and shape categories.

Analysis of movement data for the periods March–August and August–September also indicated no robust evidence of significant differences according to either clast size or shape categories, again using parametric (analysis of variance [ANOVA]) and nonparametric (Kruskal–Wallis H) analyses as appropriate (Table 4). The only exception was the Kruskal–Wallis H analysis of August–September transport distance data, grouped by clast shape categories (χ^2 [3] = 14.825, p = .002). However, this analysis included a very small sample (n = 3) for the oblate group and should, therefore, be treated with caution.

3.2 | A recovery bias in transport distance analysis?

A total of 102 (28%) of the artifacts were unrecovered after their insertion at the experimental site. To assess if artifact recovery was biased, artifact measurement means were compared with a bootstrapped

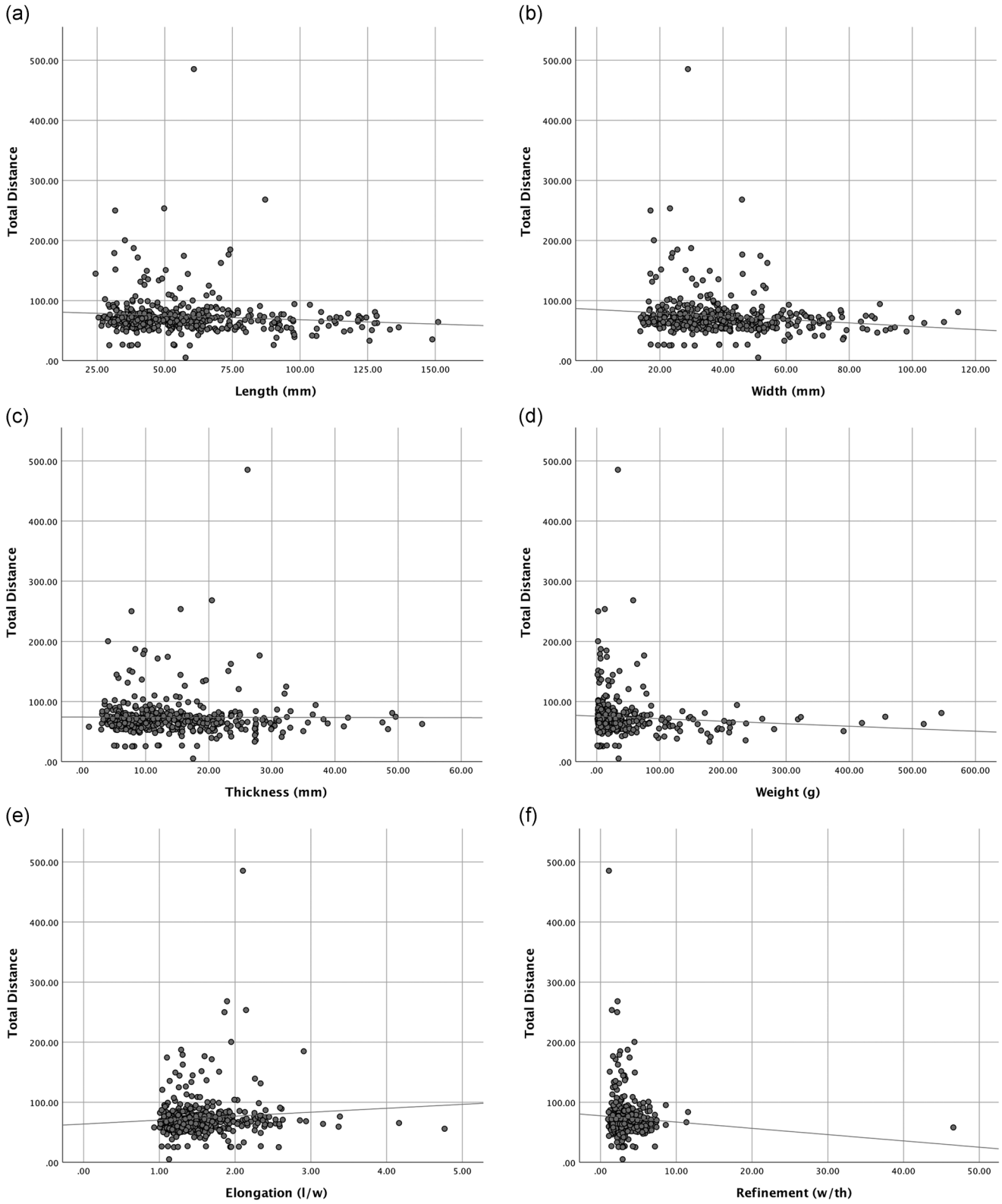

FIGURE 3 Scatter plot of artifact transport distance and (a) artifact maximum length (R^2 = .010, $F(1, 416)$ = 4.339, p < .038); (b) artifact maximum width (R^2 = .018, $F(1, 416)$ = 8.540, p < .004); (c) artifact maximum thickness (R^2 = .000, $F(1, 416)$ = 0.007, p = .932, *ns*); (d) weight; R^2 = .007, $F(1, 416)$ = 2.859, p = .092, *ns*); (e) elongation (R^2 = .007, $F(1, 416)$ = 3.068, p = .081, *ns*); (f) refinement (R^2 = .077, $F(1, 416)$ = 2.464, p = .117, *ns*). *ns*, not significant

TABLE 2 Descriptive statistics of recovered artifacts by clast size and clast shape

	Udden–Wentworth (Wentworth, 1922) grain size scheme	*n*	Minimum	Maximum	Mean	*SD*	Mean distance traveled (m)	Mean distance traveled *SD*
Length (mm)		418	40.00	151.05	64.56	22.54	73.94	35.41
	Large cobble	7	128.30	151.04	136.39	9.78	59.82	13.76
	Small cobble	150	64.04	127.70	85.19	18.13	90.55	23.74
	Very coarse pebble	261	40.00	63.97	50.77	6.96	59.38	10.89
	Coarse pebble	N/A	N/A	N/A	N/A	N/A	N/A	N/A
	Medium pebble	N/A	N/A	N/A	N/A	N/A	N/A	N/A
Width (mm)		418	14.76	114.50	43.00	17.11	73.94	35.41
	Small cobble	48	64.02	114.50	78.57	12.54	130.35	71.07
	Very coarse pebble	253	32.05	63.65	44.18	8.28	70.56	16.72
	Coarse pebble	116	16.36	31.96	25.95	3.96	58.09	16.19
	Medium pebble	1	14.76	14.76	14.76	N/A	61.85	N/A
Thickness (mm)		418	1.02	53.80	15.70	8.82	73.94	35.41
	Very coarse pebble	22	32.01	53.80	39.11	6.64	109.26	45.31
	Coarse pebble	139	16.09	31.74	22.28	4.41	88.40	49.48
	Medium pebble	189	8.06	15.94	11.65	2.30	65.13	14.77
	Fine pebble	58	4.19	7.95	6.39	1.14	58.07	11.99
	Very fine pebble	9	3.07	3.97	3.57	0.39	52.19	18.18
	Very coarse sand	1	1.02	1.02	1.02	N/A	70.96	N/A
Weight (g)		418	1.00	546	44.83	69.73	73.94	35.41

Abbreviation: *SD*, standard deviation.

independent samples *t* test, assessing if recovered and unrecovered artifacts were statistically significantly different from each other. Table 5 shows the measurements of recovered and unrecovered artifacts. Unrecovered artifacts were statistically significantly smaller by length (μ = 9 mm), width (μ = 7 mm), thickness (μ = 2 mm), and weight (μ = 21 g). Differences in measurements of transported artifacts were statistically insignificant for artifact elongation and refinement. These results suggest that the recovery of artifacts was biased towards longer, wider, thicker, and heavier artifacts and may indicate that smaller artifacts were more readily transported out of the project area.

3.3 | Where do artifacts typically become deposited in fluvial environments?

Artifacts were regularly redeposited within the center of the channel at the first river bend downstream from the point of insertion, while artifacts that were transported longer distances were typically found isolated in small (c. 50 cm in maximum dimension) scours at the margins or downstream ends of gravel bars where water velocities suddenly dropped (Figure 1). They were commonly buried within fine-grained sands and silts or found resting directly on, but embedded within, the gravel bar surfaces. This pattern was consistent during both subsequent monitoring periods.

To test potential clustering of artifacts, hot and cold spots were created using optimized hot spot analysis (OHSA; ArcMap 10.5.1). OHSA aggregates presence/absence point data and identifies statistically significant spatial clusters of high values (hot spots) and low values (cold spots), using the Getis-Ord Gi* statistic. The analysis showed that there were a greater number of significant "hot" (high value) spatial clusters in September than August (Figure 5a,b). In addition, when performed between the different shape categories (blade and oblate; Figure 5c,d) and size categories (very coarse pebble and small cobble; Figure 5e,f), the spatial distributions of high-value clusters are broadly comparable, suggesting that they did not behave any differently. It was not possible to run the analysis on the other shape categories (equant and prolate) and size categories (coarse pebble and large cobble) due to sample sizes < 60.

Artifact dispersal increased *c.* ten-fold from March to August (based on all clasts; Table 6 and Figure 6). However, the degree of spatial dispersal varied between clast size groups: from *c.* ×20 for the smallest clasts (coarse pebbles) to *c.* ×2 (large cobbles). While the samples sizes for these extreme groups were small, the data suggest a relationship between increasing artifact weight and a reduction in spatial dispersal during fluvial transport. Trends were less clear among the clast shape groups, although the prolate group showed the greatest dispersal. Since this clast shape is elongated and spherical (axis ratios: b/a < 0.67 and c/b > 0.67), it is possible that this "rugby ball" prolate shape was preferentially vulnerable to greater dispersal through a rolling motion, although this conclusion is tentative given the small sample size. The similar dispersal distances of the flattened (c/b < 0.67) oblate and bladed clasts suggest that degree of elongation (oblate: b/a > 0.67; bladed: b/a < 0.67) was not a significant factor.

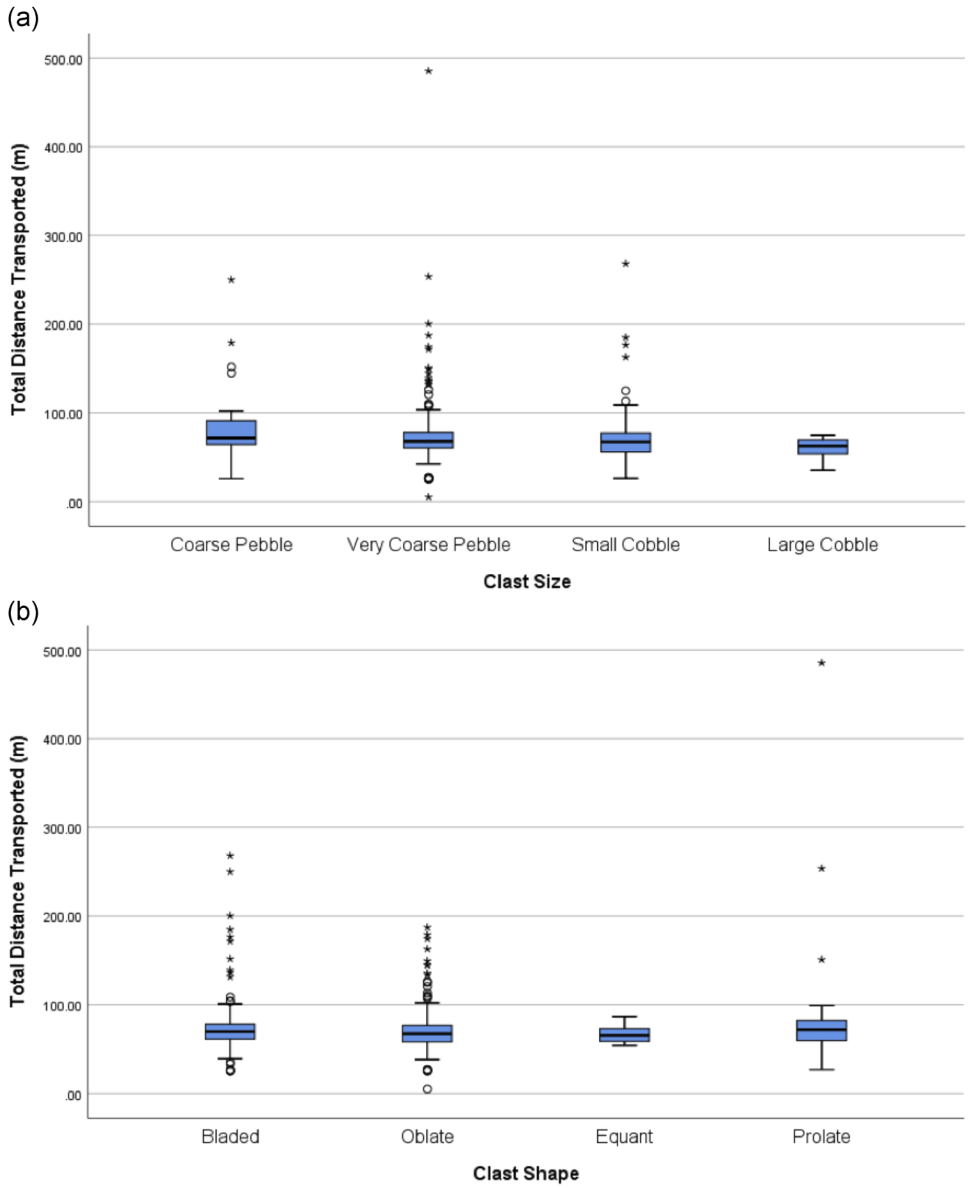

FIGURE 4 Clast transport data, (a) subdivided by clast size categories; (b) subdivided by clast shape categories. Clast sizes after the Udden–Wentworth (Wentworth, 1922) grain size scheme: coarse pebble (16–32 mm); very coarse pebble (32–64 mm); small cobble (64–128 mm); large cobble (128–256 mm; Jones, Tucker, & Hart, 1999, fig. 3.4). Artifacts defined according to largest axis. Clast shapes after Zingg (1935). Artifacts defined according to b/a and c/b ratios (Jones et al., 1999, fig. 3.6) [Color figure can be viewed at wileyonlinelibrary.com]

Changes in dispersal patterns between August and September broadly followed the March–August trends, with the exception of the coarse pebble sample (Figure 6). However, this reflects the failure to relocate the most widely (downstream) dispersed clasts in an already small sample. Small sample sizes also explain the reduced dispersal areas for the equant and large cobble samples. The general tendency towards greater dispersal of the smaller, prolate-shape clasts is supported by the degree of spatial overlap between the dispersal areas for the sample groups (Table 7): by far the largest percentages of unique dispersal areas (i.e., where there is no overlap with the other groups) occur for the prolate and coarse pebble groups, in both the August and September recording stages.

3.4 | Under what fluvial conditions is artifact orientation altered?

Artifacts were primarily buried within the river channel during the course of the experiment. Attempts to recover them required excavation, which was a time-consuming endeavor (c. 1 hr per artifact). Due to time constraints, this was seldom performed except for some of the farthest transported artifacts. When performed, the excavation process rendered orientation data unreliable due to the low visibility through the water and due to the artifacts' movement during excavation. Therefore, the number of artifacts with recognizable

TABLE 3 Clast size distributions, by clast shape categories

	Clast shape[2]								
	Bladed		Equant		Oblate		Prolate		
Clast size[1]	%[3]	*n*	%[3]	*n*	%[3]	*n*	%[3]	*n*	Total
Coarse pebble	5.4	12	0.0	0	8.8	27	3.6	1	40
Very coarse pebble	58.5	131	70.0	7	68.6	210	82.1	23	371
Small cobble	34.8	78	30.0	3	21.2	65	14.3	4	150
Large cobble	1.3	3	0.0	0	1.3	4	0.0	0	7
Total	100.0	224	100.0	10	100.0	306	100.0	28	568

[1]Clast sizes after the Udden–Wentworth (Wentworth, 1922) grain size scheme: coarse pebble (16–32 mm); very coarse pebble (32–64 mm); small cobble (64–128 mm); large cobble (128–256 mm; Jones et al., 1999, fig. 3.4). Artifacts defined according to the largest axis.
[2]Clast shapes after Zingg (1935). Artifacts defined according to b/a and c/b ratios (Jones et al., 1999, fig. 3.6).
[3]Percentages calculated for each clast shape category.

TABLE 4 Statistical analyses of movement data for the periods March–August and August–September, grouped by clast size and clast shape

Movement period	Grouping criteria	ANOVA	Kruskal–Wallis H
March–August	Clast size[1]	F (3, 283) = 3.538, p = .015[3,4]	χ^2 [3] = 6.196, p = .102
March–August	Clast shape[2]	F (3, 283) = 1.595, p = .191[3,5]	χ^2 [3] = 1.988, p = .575
August–September	Clast size[1]	F (3, 198) = 0.153, p = .928[3]	χ^2 [3] = 4.399, p = .221
August–September	Clast shape[2]	F (3, 198) = 1.084, p = .357[3]	χ^2 [3] = 14.825, p = .002

Abbreviation: ANOVA, analysis of variance.
[1]Clast sizes after the Udden–Wentworth (Wentworth, 1922) grain size scheme: coarse pebble (16–32 mm); very coarse pebble (32–64 mm); small cobble (64–128 mm); large cobble (128–256 mm; Jones et al., 1999, fig. 3.4). Artifacts defined according to largest axis.
[2]Clast shapes after Zingg (1935). Artifacts defined according to b/a and c/b ratios (Jones et al., 1999, fig. 3.6).
[3]Selected subsamples with significantly non-normal distributions (p < .05).
[4]Significant heterogeneity of variance demonstrated (p < .05); robust test results (Welch and Brown–Forsythe) nonsignificant (F_{Welch} (3, 21.906) = 2.589, p = .079; $F_{Brown-Forsythe}$ (3, 30.451) = 2.421, p = .085).
[5]Significant heterogeneity of variance demonstrated (p < .05); robust test results (Welch and Brown–Forsythe) also nonsignificant (F_{Welch} (3, 16.549) = 1.052, p = .396; $F_{Brown-Forsythe}$ (3, 21.033) = 0.767, p = .525).

TABLE 5 Descriptive statistics of recovered and unrecovered artifacts between March 2017 and September 2017

	Recovered artifacts (mean ± *SD*)	Unrecovered artifacts (mean ± *SD*)	Statistic
n	418	150	
Length (mm)	59.04 ± 25.20	49.81 ± 16.40*	t (566) = −4.176, p = .000
Width (mm)	39.89 ± 18.15	33.15 ± 12.36*	t (566) = −4.203, p = .000
Thickness (mm)	14.42 ± 8.84	12.83 ± 7.10*	t (566) = −1.991, p = .000
Weight (g)	40.14 ± 70.09	19.42 ± 27.18*	t (566) = −3.525, p = .000
Elongation	1.55 ± 0.46	1.58 ± 0.47	t (566) = 0.564, p = .573
Refinement	3.39 ± 2.59	3.14 ± 1.69	t (566) = −1.076, p = .283

Abbreviation: *SD*, standard deviation.
*p < .05 paired bootstrapped t test.

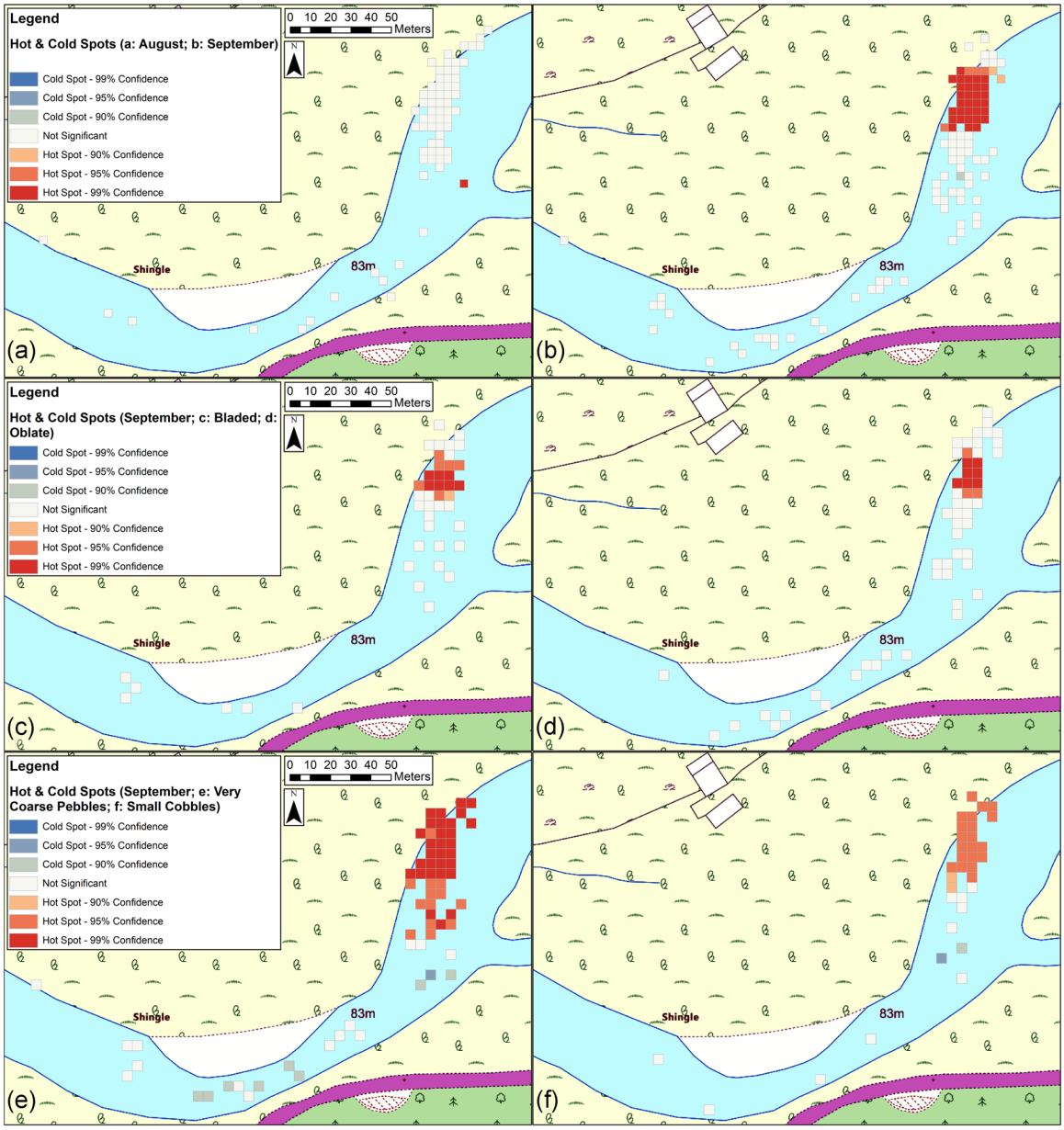

FIGURE 5 Clustering of all clasts at August (a) and September (b) recording stages. Clustering of clasts at September recording stage, subdivided by shape (c and d) and size (e and f). Hot and cold spots created using optimized hot spot analysis (OHSA; ArcMap 10.5.1). OHSA aggregates presence/absence point data and identifies statistically significant spatial clusters of high values (hot spots) and low values (cold spots), using the Getis-Ord Gi* statistic. Cells in each bin are statistically significant at the 99% (±3), 95% (±2), and 90% (±1) confidence intervals. Cell resolution: 4 m. Clast shapes after Zingg (1935). Artifacts defined according to b/a and c/b ratios (Jones et al., 1999, fig. 3.6). Clast sizes after the Udden–Wentworth (Wentworth, 1922) grain size scheme: coarse pebble (16–32 mm); very coarse pebble (32–64 mm); small cobble (64–128 mm); large cobble (128–256 mm; Jones et al., 1999, fig. 3.4). Artifacts defined according to the largest axis. Mapping: OS MasterMap 1:1,000 Raster (tiles SN7071 and SN7072). Crown copyright and database rights 2019 Ordnance Survey (100025252) [Color figure can be viewed at wileyonlinelibrary.com]

orientations ($n < 10$) was considered too small and unreliable to conduct fabric analyses (Lenoble & Bertran, 2004; McPherron, 2018).

3.5 | How does transport affect artifact damage?

All the analyzed pieces were affected by their stay in the river. Although the level of postdeposition surface modification (PDSM) varied highly, the other characteristics of the PDSM were similar between the different artifacts. The most visible aspect was the variety in size, angle, and impact angle of edge damage. The variety in impact angles (Figure 7) and the extent in the variety in direction, clearly differentiates them from use-wear or intentional retouch.

Polish was visible both along the edges and on the surface, including the ridges (Figure 7a; Figure 8). The polish was mainly formed in spots and directionality or striations were sometimes visible in the

TABLE 6 Degree of artifact concentration/dispersal, by observation period (March > August > September) and groupings (clast shape and clast size)

Recording stage	Sample groups[1,2]	Sample size	Standard distance (m)[3]	Area (m^2)
March	All clasts	453	10.50	346.41
	Bladed	176	10.66	357.30
	Equant	7	7.04	155.51
	Oblate	248	10.40	339.54
	Prolate	22	9.22	266.98
	Coarse pebble	30	10.79	365.95
	Very coarse pebble	280	10.55	349.95
	Small cobble	136	10.18	325.46
	Large cobble	7	10.62	354.40
August	All clasts	401	31.16	3,050.43
	Bladed	160	34.44	3,726.73
	Equant	8	22.21	1,549.64
	Oblate	212	25.97	2,118.08
	Prolate	21	48.87	7,501.79
	Coarse pebble	28	46.91	6,912.31
	Very coarse pebble	267	28.18	2,493.79
	Small cobble	100	30.68	2,956.61
	Large cobble	6	13.77	595.41
September	All clasts	303	43.77	6,018.98
	Bladed	118	39.74	4,960.72
	Equant	4	17.34	945.01
	Oblate	161	42.78	5,749.52
	Prolate	20	67.33	14,239.55
	Coarse pebble	20	33.72	3,571.33
	Very coarse pebble	197	47.07	6,959.48
	Small cobble	82	37.12	4,328.54
	Large cobble	4	7.24	164.87

[1]Clast sizes after the Udden–Wentworth (Wentworth, 1922) grain size scheme: coarse pebble (16–32 mm); very coarse pebble (32–64 mm); small cobble (64–128 mm); large cobble (128–256 mm; Jones et al., 1999, fig. 3.4).
[2]Clast shapes after Zingg (1935). Artifacts defined according to b/a and c/b ratios (Jones et al., 1999, fig. 3.6).
[3]Standard Distance statistics generated using *Standard Distance* analysis in ArcMap 10.5.1; standard distance = circle radius (circle size set at 1 standard deviation; i.e., *c.* 63% of data points).

polish. This directionality varied between the different spots (Figure 7b; Figure 9a). The polish was not observed directly on the edge but was found spread both along and away from the edge. This polish was disordered, varied in texture, and lacked indicative characteristics. The polish was generally better developed on protruding parts, for example, the ridges (*arêtes*). All of these characteristics clearly distinguished these traces from anthropogenic use-wear traces. Where residual use-wear traces from the previous butchery experiments were still visible, these were partially obscured by the PDSMs, but were still clearly distinguishable (Figure 9). On many of the pieces, rounding from the current experiments was also visible. Generally, it was only lightly developed along the edges, but more strongly developed on the ridges and protruding parts of the artifacts (Figure 9).

4 | DISCUSSION

4.1 | Relating the results to previous experiments

Between March 2017 and September 2017, artifacts were transported an average of 73.94 ± 35.41 m and were recovered at a rate of 72%; both of these figures are significantly better than previously reported experiments suggesting that RFID tagging of artifacts is an effective method of recovering transported experimental materials.

The results of the bootstrapped linear regressions showed that transport distance was significantly predicted by maximum length ($R^2 = 0.010$; Figure 3; $p < .05$) and maximum width ($R^2 = 0.020$; Figure 3; $p < .05$) though the R^2 values are low suggesting that other factors are involved in artifact transport. Weight, thickness, elongation, and refinement were statistically insignificant predictors of artifact transport (Figure 3; $p > .05$). These results suggest that transport distances of lithic artifacts in gravel-bedded rivers are partially, albeit weakly, dependent on overall length, and width of artifacts. Shorter, narrower artifacts tend to be transported farther than longer and wider artifacts. The results also indicate that weight and thickness are not significant predictors of artifact transport, suggesting that artifact transport is better predicted by overall dimensions than weight (Byers et al., 2015; Hosfield & Chambers, 2004a). Given that unrecovered artifacts were consistently smaller than recovered artifacts, and that this may in part be due to them being transported out of the experimental area, the effect of size on transport distance may be under-reported. Elongation and thickness were also insignificant predictors of artifact transport distances indicating that "dimensionless" artifact shapes (e.g., short squat flakes or long thin flakes) did not play a statistically significant role in transport. The results of the Kruskal–Wallis and ANOVAs showed that transport distance were not significantly different when grouped by artifacts size and shape classes regardless of monitoring periods which had different maximum discharges.

The results of the OHSA showed a greater number of significant "hot" (high value) spatial clusters in September than August (Figure 5a,b). This is likely because more of the August scatters were concentrated in the same location (close to the insertion point) and thus relatively few hot spots. By contrast, as the material became more dispersed in September, the hot spots (still close to the insertion point) were more apparent.

Interestingly, while previous experiments have reported correlations between artifact dimensions, artifact types, and horizontal displacement (Chu, 2016; Harding et al., 1987; Isaac, 1967; Petraglia & Nash, 1987, p. 69; Schick, 1986, p. 79), others have not (Hosfield & Chambers, 2004a). This study agrees with the former studies where smaller flakes moved longer distances. Though clast dimensions are

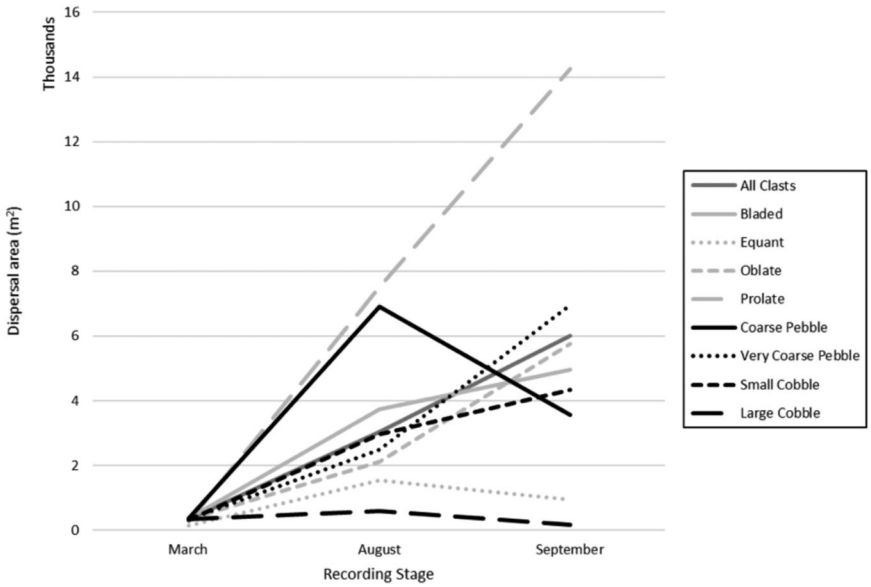

FIGURE 6 Degree of artifact concentration/dispersal, by observation period (March > August > September) and groupings (clast shape and clast size). Clast sizes after the Udden–Wentworth (Wentworth, 1922) grain size scheme: coarse pebble (16–32 mm); very coarse pebble (32–64 mm); small cobble (64–128 mm); large cobble (128–256 mm; Jones et al., 1999, fig. 3.4); Clast shapes after Zingg (1935). Artifacts defined according to b/a and c/b ratios (Jones et al., 1999, fig. 3.6). Dispersal area data calculated from Standard Distance statistics, generated using *Standard Distance* analysis in ArcMap 10.5.1; standard distance = circle radius (circle size set at 1 standard deviation; i.e. *c.* 63% of data points). For sample sizes see Table 6. One data point was not included in this analysis for March due to imprecise GPS coordinates. GPS, global positioning system

intimately related to each other, the results of this study confirm that length and width are better predictors of transport distance than weight (Wilcock, 1997). However, while the relationships are statistically significant, the R^2 values for length and width are low (0.010 and 0.020, respectively) indicating that artifact size accounts for < 2% of variation in transport distance.

The differences between this study's results and those of Hosfield and Chambers (2005) are probably in part due to their lower

TABLE 7 Degree of spatial separation/overlap between artifacts, by observation period (August and September) and groupings (clast shape and clast size)

Recording stage	Sample group	Sample size	Unique dispersal area (%)	Shared (with 1/2 other categories)	Shared with all other categories
August	Bladed	160	0.0	62.0	38.0
	Equant	8	0.0	8.5	91.5
	Oblate	212	0.0	33.1	66.9
	Prolate	21	50.3	30.8	18.9
	Coarse pebble	28	54.3	42.9	2.8
	Very coarse pebble	267	0.0	92.3	7.7
	Small cobble	100	3.0	90.5	6.5
	Large cobble	6	8.8	58.7	32.4
September	Bladed	118	0.0	81.0	19.0
	Equant	4	0.0	0.0	100.0
	Oblate	161	0.0	83.6	16.4
	Prolate	20	59.6	33.7	6.6
	Coarse pebble	20	0.0	95.4	4.6
	Very coarse pebble	197	30.4	67.3	2.4
	Small cobble	82	0.0	96.2	3.8
	Large cobble	4	0.0	0.0	100.0

Note: Clast sizes after the Udden–Wentworth (Wentworth, 1922) grain size scheme: coarse pebble (16–32 mm); very coarse pebble (32–64 mm); small cobble (64–128 mm); large cobble (128–256 mm; Jones et al., 1999, fig. 3.4); Clast shapes after Zingg (1935). Artifacts defined according to b/a and c/b ratios (Jones et al., 1999, fig. 3.6).

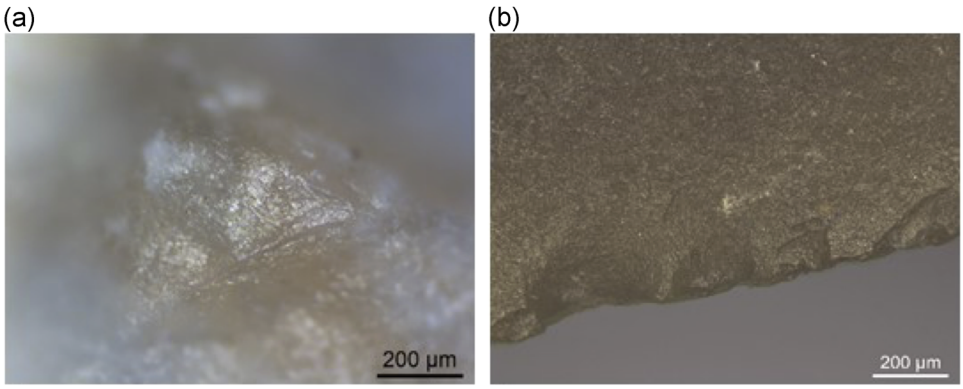

FIGURE 7 (a) Rounded protrusion with polish and striations on artifact #99 (transported 485 m; (b) edge damage with high impact angles and varying scar size and directionality (artifact #305; transported 200 m) [Color figure can be viewed at wileyonlinelibrary.com]

recovery rates but also to the longer timescale of their study that may have provided more opportunities for the materials to become mobile, including larger artifacts (Ferguson & Hoey, 2002; Ferguson, Bloomer, Hoey, & Werritty, 2002). This study used handaxes, flakes, and blades but the output regimen of the Ystwyth was never above 30 m^3/s, while between 2000 and 2003 (Hosfield & Chambers 2004a) river discharge reached a maximum of 75.62 m^3/s. Hosfield and Chambers' (2004a) finding of an insignificant relationship between artifact length, width, and thickness and horizontal displacement may, therefore, be the result of an output regimen too extreme to discriminate between small ranges of artifact sizes.

Many previous studies provide data allowing for direct comparison of horizontal displacement of artifacts and the results of this experiment are within these reported ranges. Among artifacts deposited on the riverbanks (Stations E and H) Petraglia & Nash (1987) reported that scatters were buried "in situ." Schick (1986) also reported seven experiments (Sites 3a–3b, 14–15, 25, 28, and 34) where artifacts emplaced on the banks of rivers were "minimally disturbed" (i.e., artifacts stayed mostly in place with a maximum transport of 7 m). However, Schick (1986) described other bankside experiments (Sites 13 and 20–22) as more heavily modified, reporting that transport values increased to as far as 19 m in one case. These differences were attributed to scatters being located lower and closer to the active channel than other scatters (Schick, 1987).

Experiments such as the current one where artifacts were placed within an active channel (either directly or on a bar) showed greater transport distances. Schick (1986) found that such sites were scoured, truncated, or experienced "major disturbance," resulting in transport of up to 90 m (Sites 1c, 3a–3b, 19, 23, 24, 26–27, and 36). Petraglia and Nash (1987) reported similar results (Stations C and D) with in-channel artifacts dispersed up to an average of 33.1 m. Hosfield and Chambers (2004a) reported a maximum transport distance of 84.95 m while Harding et al. (1987) observed variable disturbance with some artifacts not moving at all, while others were transported up to 150 m. Only Isaac (1967) reported minor horizontal movement of his in-channel artifact scatters, though a likely reason for this and the variable distances of Harding et al. (1987) was their use of heavier, less mobile handaxes compared to the predominantly flake-based assemblages of this and other experiments. Transport distances in previous experiments were lower than this study's maximum transport distance of 485 m, however, this is likely the result of variable artifact recovery methods as, where reported, river discharge was always higher in the other experiments and the experimental durations were also longer in those experiments. A further factor may be this study's use of the "riverdist" package to measure transported distances, as opposed to linear, straight-line measurements between observation points that were used, for example, in Hosfield and Chambers (2004a).

Comparing discharge values of the River Ystwyth to those of other rivers used in earlier experiments indicates that daily mean flow and average flows were low compared with those previously reported, though the high flows for this study of 30 m^3/s were comparable with those of Petraglia and Nash (1987) and Chu (2016). An estimate of river flashiness, calculated as mean daily flow/maximum discharge, showed that during this experiment, the Ystwyth was the least flashy of all the rivers. Synthesizing this study with others is difficult because other authors do not report associations with fluvial output and differences in assemblage composition and artifact recovery rates, making straightforward comparisons untenable. Understanding the impact of flow, therefore, remains an outstanding question for future research. Nevertheless, this study does identify a new minimum fluvial output regime for transporting artifacts of 30 m^3/s. This suggests that the exposure of artifacts to active flows in smaller, meandering channels such as the Ystwyth can still have deleterious effects on archaeological assemblages.

4.2 | Archaeological context

Though archaeologists working on lithic assemblages in fluvial settings from Northern Europe have long been aware of the influences of natural processes in forming spatial patterns (e.g., Evans, 1862; Passmore et al., 2011; White, Scott, & Ashton, 2006), not enough appreciation has

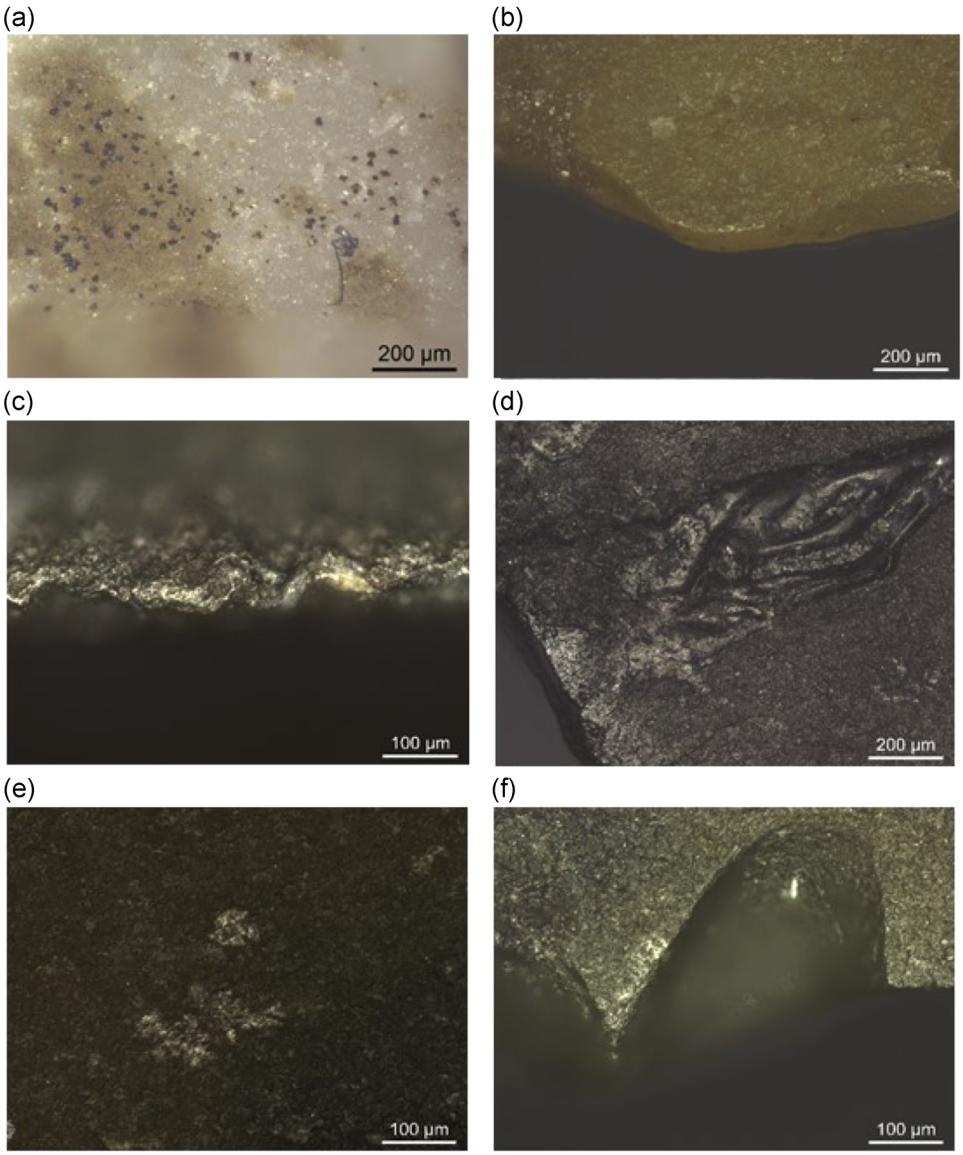

FIGURE 8 (a) Small black dots on the surface of artifact #107 (transported > 10 m); (b) polish development along the edge of artifact #194 (transported 194 m); (c) use-wear traces with a transverse directionality on artifact #259 (transported 75 m); (d) black residue on artifact #305 (transported 200 m); (e) highly reflective polish with directionality on artifact #305; (f) microscopic linear impact trace connected to a retouch on artifact #305 [Color figure can be viewed at wileyonlinelibrary.com]

been paid to the exact character of the disturbances by fluvial processes in both primary and secondary archaeological contexts. The way in which archaeological material can be dispersed in fluvial deposits is of considerable interest to Paleolithic archaeologists because it can obscure anthropogenic spatial patterns and alter their morphology. Understanding the specifics of fluvial disturbance is perhaps especially critical in the case of small-scale disturbances of primary context assemblages, where the physical indicators of transport are likely to be subtler but the consequence for behavioral interpretations is nonetheless important. Previous researchers have suggested that fluvial site disturbance can be identified by comparing size distributions of artifacts to the results of experimental fluvial disturbances of "control" assemblages derived from experimental knapping events (Bertran, Lenoble, Todisco, Desrosiers, & Sørensen, 2012; Dibble, Chase, McPherron, & Tuffreau, 1997; Petraglia & Potts, 1994; Schick, 1986; de la Torre et al., 2018). The absence of smaller artifacts after fluvial disturbance that has been recorded in some experiments of this kind has generally been interpreted as a possible indication of downstream fining and a potential means of detecting archaeological assemblage reworking (Isaac, 1967; Malinsky-Buller, Hovers, & Marder, 2011; Schick, 1987; de la Torre et al., 2018). Other experiments, however, have found no such association, suggesting that artifact dispersal is a highly complicated process influenced by the river's output regimen (Petraglia & Nash, 1987), the discard location of the artifacts (Dennell, 2004; Harding et al., 1987, p. 250), and the nature of the bedload/rugosity (Hosfield & Chambers, 2004a). This experiment has broadly, but not conclusively, supported the former view, highlighting

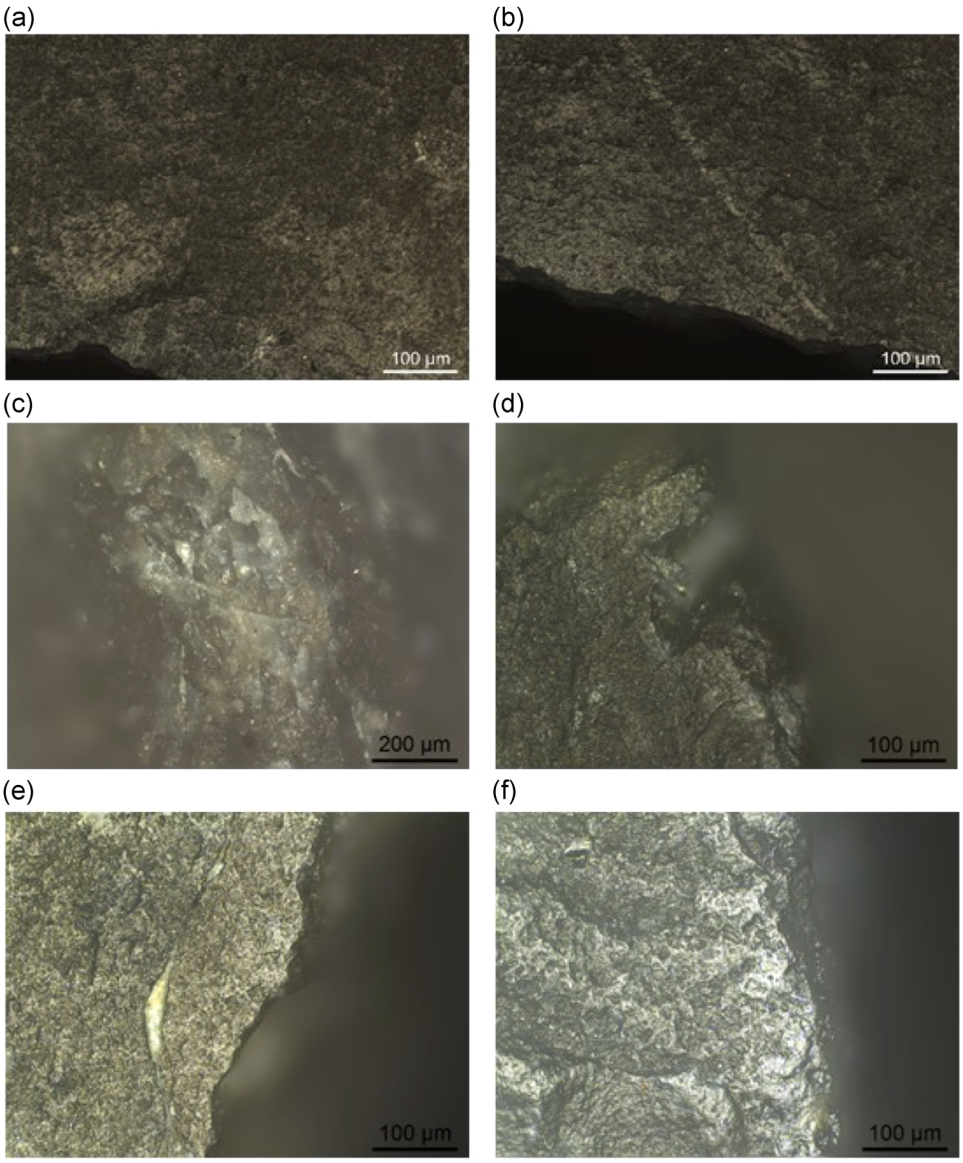

FIGURE 9 (a) Spots of polish with a varying directionality on artifact #528 (transported 87 m); (b) scratch on the surface of artifact #528; (c) impact traces on the surface of artifact #704 (transported > 10 m); (d) traces of the hammer used in a series of failed retouches on artifact #704; (e) use-wear traces, probably the result of working an animal material; (f) possible use-wear traces on the tip of artifact #704 [Color figure can be viewed at wileyonlinelibrary.com]

trends in (a) artifact size in a downstream direction from the assemblage source; (b) the development of distinctive PDSM traces over tens and hundreds of meters, and (c) patterns in artifact depositional locations after transport.

4.3 | Limitations and future work

The application of the Ystwyth experiment to the Paleolithic record has some limitations due to the scope of the experiment. However, some of these may be overcome through further work:

First, the short duration of the tracer studies gives insufficient information about the long-term/long-range effects of artifact transport, although this may be partially overcome by longer artifact transport studies combined with improved theoretical models (Hassan, Church, & Ashworth, 1992; Klösch & Habersack, 2018; Milan, 2013).

Second, these experiments only examined a single river type and their application to Pleistocene river types is therefore limited to comparable settings.

Third, artifact transport and modification patterns are based on a maximum transport distance of 485 m, and thus may be principally relevant to locally disturbed sites. Therefore, these results should not be generalized to more heavily transported data sets as longer transport periods may generate different results.

Fourth, there are undoubtedly more variables involved in artifact fluvial transport that require exploration, notably channel morphology,

riparian vegetation cover, and bankside erosion rates (Ashton, Lewis, Parfitt, & White, 2006; Hassan & Bradley, 2017; Vázquez-Tarrío, Recking, Liébault, Tal, & Menéndez-Duarte, 2019).

Fifth, microwear still remains a largely subjective appraisal however future advances in quantitative microscopy and tribology may help to accurately assess taphonomic signatures (Stemp, 2018).

Finally, active RFID and tracer systems may clarify the ultimate locations of artifacts outside search areas and be able to identify the exact timing and distance of their movements with reference to flow regimes (Cassel, Dépret, & Piégay, 2017).

5 | CONCLUSION

Particle kinematics in gravel-bed rivers is a complex process, whereby sedimentological and geomorphological controls are superimposed on the hydraulic forcing (Vázquez-Tarrío et al., 2019). Still, this study has demonstrated a significant and robust association between sedimentary factors and artifact transport, most notably, the weak association of artifact size with transport distance. It has also confirmed the association of short distance/short period transport with the development of microwear. The study has neither conclusively proven nor falsified previous hypotheses concerning the nature of fluvial site formation processes. It has, however, highlighted the complex nature of alluvial site formation processes in a repeatable experiment featuring the transport of replica Paleolithic material. It examined artifact dimensions and river discharge and demonstrated their relevance to the transport of flint artifacts. It also identified that in a gravel-bedded regimen, morphological characteristics such as edge and surface condition and assemblage size distributions may provide details about artifact life-histories.

ACKNOWLEDGMENTS

W. Chu is funded by the Deutsche Forschungsgemeinschaft (DFG, German Research Foundation), project number 57444011 - SFB 806. Experimental costs were provided by a Postdoc Grant funded through the Institutional Strategy of the University of Cologne (Excellence Initiative). We would like to thank Attila Király, György Lengyel, Anna Machin, and Zoltán Tóth for furnishing knapped materials used in this experiment. We are also grateful to Gregory Grumann, Olivia Morton, and Laurenz Rathke for their help with sample preparation and fieldwork. Paul Wright was helpful in providing DEMs of the area. Thank you to Andreas Bolten for help with creating the map figures. Thank you also to Radu Iovițǎ and the Department of Anthropology at New York University for hosting W. Chu during which time this article was written.

CONFLICT OF INTERESTS

The authors declare that there are no conflict of interests.

ORCID

Wei Chu http://orcid.org/0000-0002-4595-388X
Robert Hosfield http://orcid.org/0000-0001-6357-2805

REFERENCES

Andrefsky, W. (2005). *Lithics macroscopic approaches to analysis* (2nd ed.). Cambridge, UK; New York, NY: Cambridge University Press.

Ashton, N., Lewis, S. G., Parfitt, S. A., & White, M. J. (2006). Riparian landscapes and human habitat preferences during the Hoxnian (MIS 11) Interglacial. *Journal of Quaternary Science*, *21*, 497–505.

Bertran, P., Bordes, J.-G., Todisco, D., & Vallin, L. (2017). TaphonomieS. Ouvrage du groupement de recherches «taphonomie, environnement et archéologie», CNRS-INEE. In J.-P Brugal (Ed.), *Géoarchéologie et taphonomie des vestiges archéologiques: Impacts des processus naturels sur les assemblages et méthodes d'analyse* (pp. 123–156). Paris: Editions des Archives Contemporaines.

Bertran, P., Lenoble, A., Todisco, D., Desrosiers, P. M., & Sørensen, M. (2012). Particle size distribution of lithic assemblages and taphonomy of Palaeolithic sites. *Journal of Archaeological Science*, *39*, 3148–3166.

van den Biggelaar, D. F. A. M., Balen, R. T., van, Kluiving, S. J., Verpoorte, A., & Alink, G. M. (2017). Gravel size matters: Early Middle Palaeolithic artefacts made from local Rhine and Meuse deposits in the central Netherlands. *Netherlands Journal of Geosciences*, *96*, 261–271.

Brewer, P. A., Johnstone, E., & Macklin, M. (2009). River dynamics and environmental change in Wales. In D. D. Williams & C. A. Duigan (Eds.), *The rivers of Wales* (pp. 17–34). Leiden, Netherlands: Backhuys.

Brewer, P. A., Maas, G. S., & Macklin, M. G. (2001). *A fifty-year history of exposed riverine sediment dynamics*. In: Water in the Celtic world: Managing resources for the 21st century (pp. 245–252). British Hydrological Society, Occasional paper.

Bridgland, D. R. (2000). River terrace systems in north-west Europe: An archive of environmental change, uplift and early human occupation. *Quaternary Science Reviews*, *30*, 1293–1303.

Bridgland, D. R., Antoine, P., Limondin Lozouet, N., Santisteban, J., Westaway, R., & White, M. J. (2006). The Palaeolithic occupation of Europe as revealed by evidence from the rivers: Data from IGCP 449. *Journal of Quaternary Science*, *21*, 437–455.

Bridgland, D. R., & White, M. J. (2014). Fluvial archives as a framework for the Lower and Middle Palaeolithic: Patterns of British artefact distribution and potential chronological implications. *Boreas*, *43*, 543–555.

Bunn, H., Harris, J. W. K., Isaac, G., Kaufulu, Z., Kroll, E., Schick, K., … Behrensmeyer, A. (1980). FxJj50: An Early Pleistocene site in Northern Kenya. *World Archaeology*, *12*, 109–136.

Byers, D. A., Hargiss, E., & Finley, J. B. (2015). Flake morphology, fluvial dynamics, and debitage transport potential. *Geoarchaeology*, *30*, 379–392.

Cassel, M., Dépret, T., & Piégay, H. (2017). Assessment of a new solution for tracking pebbles in rivers based on active RFID. *Earth Surface Processes and Landforms*, *42*, 1938–1951.

Cassel, M., Piégay, H., & Lavé, J. (2017). Effects of transport and insertion of radio frequency identification (RFID) transponders on resistance and shape of natural and synthetic pebbles: Applications for riverine and coastal bedload tracking. *Earth Surface Processes and Landforms*, *42*, 399–413.

Chambers, J. C. (2004). River gravels and handaxes: New experiments in site formation, stone tool transportation and transformation. In M. Fansa (Ed.), *Experimentelle archäologie in Europa, bilanz* (pp. 25–41). Oldenburg, Germany: Isensee Verlag.

Chapuis, M., Bright, C. J., Hufnagel, J., & MacVicar, B. (2014). Detection ranges and uncertainty of passive Radio Frequency Identification (RFID) transponders for sediment tracking in gravel rivers and coastal environments. *Earth Surface Processes and Landforms*, *39*, 2109–2120.

Chauhan, P. R., Bridgland, D. R., Moncel, M.-H., Antoine, P., Bahain, J.-J., Briant, R., … Locht, J.-L. (2017). Fluvial deposits as an archive of early human activity: Progress during the 20 years of the Fluvial Archives Group. *Quaternary Science Reviews*, *166*, 114–149.

Chu, W. (2016). *Fluvial processes in the Pleistocene of Northern Europe*. Oxford, UK: BAR International Series.

Dennell, R. (2004). *Early hominin landscapes in Northern Pakistan: Investigations in the Pabbi Hills*. Oxford, UK: BAR International Series.

Dibble, H. L., Chase, P. G., McPherron, S. P., & Tuffreau, A. (1997). Testing the reality of a "living floor" with archaeological data. *American Antiquity*, *62*, 629–651.

Ditchfield, K. (2016). An experimental approach to distinguishing different stone artefact transport patterns from debitage assemblages. *Journal of Archaeological Science*, *65*, 44–56.

Eren, M. I., Lycett, S. J., Patten, R. J., Buchanan, B., Pargeter, J., & O'Brien, M. J. (2016). Test, model, and method validation: The role of experimental stone artifact replication in hypothesis-driven archaeology. *Ethnoarchaeology*, *8*, 103–136.

Evans, J. (1862). *Flint implements in the drift: Being an account of further discoveries on the continent and in England, communicated to the Society of Antiquaries*. London, UK: J. B. Nichols and Sons.

Ferguson, R. I., Bloomer, D. J., Hoey, T. B., & Werritty, A. (2002). Mobility of river tracer pebbles over different timescales. *Water Resources Research*, *38*, 3–8.

Ferguson, R. I., & Hoey, T. B. (2002). Long-term slowdown of river tracer pebbles: Generic models and implications for interpreting short-term tracer studies. *Water Resources Research*, *38*(8), 1142.

Foulds, S. A., Griffiths, H. M., Macklin, M. G., & Brewer, P. A. (2014). Geomorphological records of extreme floods and their relationship to decadal-scale climate change. *Geomorphology*, *216*, 193–207.

van Gijn, A. L. (1989). *The wear and tear of flint: Principles of functional analysis applied to Dutch Neolithic assemblages*. Leiden, Netherlands: University of Leiden.

van Gijn, A. L. (2010). *Flint in focus: Lithic biographies in the Neolithic and Bronze Age*. Leiden, Netherlands: Sidestone Press.

Graham, D. J., Reid, I., & Rice, S. P. (2005). Automated sizing of coarse-grained sediments: Image-processing procedures. *Mathematical Geology*, *37*, 1–28.

Graham, D. J., Rice, S. P., & Reid, I. (2005). A transferable method for the automated grain sizing of river gravels. *Water Resources Research*, *41*(7), W07020.

Harding, P., Gibbard, P. L., Lewin, J., Macklin, M. G., & Moss, E. H. (1987). The transport and abrasion of flint handaxes in a gravel-bed river. In G. De G. Sieveking & M. H. Newcomer (Eds.), *The human uses of flint and chert* (pp. 115–126). Cambridge UK: Cambridge University Press.

Hassan, M. A., & Bradley, D. N. (2017). Geomorphic controls on tracer particle dispersion in gravel-bed rivers. In D. Tsutsumi & J. B. Laronne (Eds.), *Gravel -bed rivers* (pp. 159–184). Chichester, UK: John Wiley & Sons, Ltd.

Hassan, M. A., Church, M., & Ashworth, P. (1992). Virtual rate and mean distance of travel of individual clasts in gravel-bed channels. *Earth Surface Processes and Landforms*, *17*, 617–627.

Hosfield, R. T. (2011). Rolling stones: Understanding river-rolled Paleolithic artifact assemblages. *Geological Society of America, Special Papers*, *476*, 37–52.

Hosfield, R. T., & Chambers, J. (2004a). River gravels and flakes: New experiments in site formation, stone tool transportation and transformation. In M. Fansa (Ed.), *Experimentelle archäologie in Europa, bilanz* (pp. 57–74). Oldenburg, Germany: Isensee Verlag.

Hosfield, R. T., & Chambers, J. (2004b). Experimental archaeology on the Afon Ystwyth, Wales, UK. *Antiquity*, *78*.

Hosfield, R. T., & Chambers, J. (2005). Flake modifications during fluvial transportation: Three cautionary tales. *Lithics: The Newsletter of the Lithic Studies Society*, *24*, 57–65.

Hosfield, R. T., Chambers, J. C., Macklin, M. G., Brewer, P. A., & Sear, D. (2000). Interpreting secondary context sites: A role for experimental archaeology. *Lithics: The Newsletter of the Lithic Studies Society*, *21*, 29–35.

Houbrechts, G., Levecq, Y., Peeters, A., Hallot, E., Van Campenhout, J., Denis, A. -C., & Petit, F. (2015). Evaluation of long-term bedload virtual velocity in gravel-bed rivers (Ardenne, Belgium). *Geomorphology*, *251*, 6–19.

Iovita, R., & McPherron, S. P. (2011). The handaxe reloaded: A morphometric reassessment of Acheulian and Middle Paleolithic handaxes. *Journal of Human Evolution*, *61*, 61–74.

Isaac, G. (1967). Towards the interpretation of occupation debris: Some experiments and observations. *Kroeber Anthropological Society Papers*, *37*, 31–57.

Jones, A. P., Tucker, M. E., & Hart, J. K. (1999). Guidelines and recommendations. In A. P. Jones, M. E. Tucker & J. K. Hart (Eds.), *The description & analysis of quaternary stratigraphic field sections*. London, UK: Quaternary Research Association. (Technical Guide No. 7).

Klösch, M., & Habersack, H. (2018). Deriving formulas for an unsteady virtual velocity of bedload tracers. *Earth Surface Processes and Landforms*, *43*, 1529–1541.

Lamarre, H. (2005). Using passive integrated transponder (PIT) tags to investigate sediment transport in gravel-bed rivers. *Journal of Sedimentary Research*, *75*, 736–741.

Lengyel, G., & Chu, W. (2016). Long thin blade production and Late Gravettian hunter-gatherer mobility in Eastern Central Europe. *Quaternary International*, *406*, 166–173.

Lenoble, A., & Bertran, P. (2004). Fabric of Palaeolithic levels: Methods and implications for site formation processes. *Journal of Archaeological Science*, *31*, 457–469.

Lewin, J., Bradley, S. B., & Macklin, M. G. (1983). Historical valley alluviation in mid-Wales. *Geological Journal*, *18*, 331–350.

Lin, S. C., Rezek, Z., & Dibble, H. L. (2018). Experimental design and experimental inference in stone artifact archaeology. *Journal of Archaeological Method and Theory*, *25*, 663–688.

Machin, A. J., Hosfield, R. T., & Mithen, S. J. (2007). Why are some handaxes symmetrical? Testing the influence of handaxe morphology on butchery effectiveness. *Journal of Archaeological Science*, *34*, 883–893.

Malinsky-Buller, A., Hovers, E., & Marder, O. (2011). Making time: 'Living floors', 'palimpsests' and site formation processes - A perspective from the open-air Lower Paleolithic site of Revadim Quarry, Israel. *Journal of Anthropological Archaeology*, *30*, 89–101.

McPherron, S. P. (2018). Additional statistical and graphical methods for analyzing site formation processes using artifact orientations. *PLoS One*, *13*, e0190195.

Milan, D. J. (2013). Virtual velocity of tracers in a gravel-bed river using size-based competence duration. *Geomorphology*, *198*, 107–114.

Passmore, D. G., Waddington, C., van der Schriek, T., Davis, B., Tetlow, E., Smith, D., & Cotton, J. (2011). Geoarchaeology and archaeological landscapes in the Till River Valley, northern England. *Geological Society of America, Special Papers*, *476*, 117–133.

Petraglia, M. D., & Nash, D. (1987). The impact of fluvial processes on experimental sites. In D. Nash & M. D. Petraglia (Eds.), *Natural formation processes and the archaeological record* (pp. 108–130). Oxford, UK: BAR International Series.

Petraglia, M. D., & Potts, R. (1994). Water flow and the formation of Early Pleistocene artifact sites in Olduvai Gorge, Tanzania. *Journal of Anthropological Archaeology*, *13*, 228–254.

Schick, K. D. (1986). *Stone age sites in the making: Experiments in the formation and transformation of archaeological occurrences*. Oxford, UK: BAR International Series.

Schick, K. D. (1987). Experimentally-derived criteria for assessing hydrological disturbances of archaeological sites. In D. Nash & M. D. Petraglia (Eds.), *Natural formation processes and the archaeological record*. Oxford, UK: BAR International Series.

Stemp, W. J. (2018). Lithics data quantification. In S. L. López (Ed.), *The Encyclopedia of Archaeological Sciences*. Malden, MA: John Wiley & Sons.

de la Torre, I., Benito-Calvo, A., & Proffitt, T. (2018). The impact of hydraulic processes in Olduvai Beds I and II, Tanzania, through a particle dimension analysis of stone tool assemblages. *Geoarchaeology*, *33*, 218–236.

Vázquez-Tarrío, D., Recking, A., Liébault, F., Tal, M., & Menéndez-Duarte, R. (2019). Particle transport in gravel-bed rivers: Revisiting passive tracer data. *Earth Surface Processes and Landforms*, *44*, 112–128.

Wentworth, C. K. (1922). A scale of grade and class terms for clastic sediments. *Journal of Geology*, *30*, 377–392.

Westaway, R., Bridgland, D. R., Sinha, R., & Demir, T. (2009). Fluvial sequences as evidence for landscape and climatic evolution in the Late Cenozoic: A synthesis of data from IGCP 518. *Global and Planetary Change*, *68*, 237–253.

White, M., Scott, B., & Ashton, N. (2006). The Early Middle Palaeolithic in Britain: Archaeology, settlement history and human behaviour. *Journal of Quaternary Science*, *21*, 525–541.

Wilcock, P. (1997). Entrainment, displacement and transport of tracer gravels. *Earth Surface Processes and Landforms*, *22*, 1125–1138.

Zingg, T. H. (1935). Beiträge zur schotteranalyse. *Schweizerische Mineralogische und Petrographische Mitteilungen*, *15*, 39–140.

How to cite this article: Chu W, Hosfield R. Lithic artifact assemblage transport and microwear modification in a fluvial setting: A radio frequency identification tag experiment. *Geoarchaeology*. 2020;35:591–608. https://doi.org/10.1002/gea.21788